

Title

kTMP: A New Non-invasive Magnetic Induction Method to Modulate Cortical Excitability.

Author names and affiliations

Ludovica Labruna^{*1-2}, Christina Merrick^{*1-2}, Ben Inglis², Richard Ivry¹⁻², Daniel Sheltraw¹⁻²

¹Department of Psychology and, ²Helen Wills Neuroscience Institute, University of California, 94704 Berkeley, California; ^{*}co-first authors.

Corresponding author: Ludovica Labruna, Department of Psychology, 3002 Berkeley Way, University of California, Berkeley, CA 94704, email: lulabrun@gmail.com.

Abstract

We report a novel subthreshold non-invasive brain stimulation approach that we refer to as kilohertz transcranial magnetic perturbation, or kTMP. kTMP is a magnetic induction method that delivers kHz-frequency cortical E-fields and, through amplitude modulation of the kHz carrier frequency, may mimic E-fields at physiological frequencies. To evaluate the efficacy of kTMP, we used suprathreshold TMS to elicit motor-evoked potentials (MEP) in a peripheral muscle, comparing the amplitude of the MEPs before and after kTMP stimulation. In Experiment 1, we used non-modulated kTMP with an E-field amplitude of 2 V/m over motor cortex. Ten minutes of kTMP stimulation resulted in an increase in cortical excitability in a frequency-specific manner. We replicated this effect in Experiment 2 and found that amplitude-modulation at 20 Hz produced an additional boost in cortical excitability. The only percept associated with kTMP is a faint auditory tone, making kTMP ideal for double-blind experimentation.

Keywords: non-invasive brain stimulation, high frequency magnetic induction, electric field, amplitude modulation

Introduction

Non-invasive brain stimulation (NIBS) is a group of methods which perturb brain function by coupling an applied electric field (E-field) to the tissue of the brain without the need to invasively introduce electrodes. The NIBS E-field can safely manipulate neural excitability, providing neuroscientists with a powerful tool to advance our understanding of brain function. Evidence that NIBS can promote brain plasticity¹ has prompted clinicians to pursue NIBS interventions in the treatment of psychiatric and neurologic disorders²⁻⁷.

The NIBS E-field amplitude can be categorized as subthreshold or suprathreshold. Suprathreshold fields are sufficient to elicit immediate action potentials in neurons near resting membrane potential. Subthreshold E-fields are insufficient to directly cause action potentials but may alter the state of the targeted neurons on time scales ranging from immediate entrainment effects to plasticity effects that extend well past the stimulation epoch^{8,9}. As such subthreshold and suprathreshold methods have different experimental utilities.

Two broad categories of NIBS methods exist: Electrical contact methods (EC) and magnetic induction methods (MI). EC methods such as transcranial electric stimulation (tES) establish a cortical E-field via electrodes in contact with the scalp. In tES, the current is either constant as in transcranial direct current stimulation (tDCS) or time varying as in transcranial alternating current stimulation (tACS). MI methods, such as transcranial magnetic stimulation (TMS), establish a cortical E-field via a current-carrying coil that is positioned near the scalp, generating a time-varying magnetic field and consequently an induced cortical E-field. TMS is delivered as a brief pulse (typically 200-300 μ s) and is referred to as repetitive TMS (rTMS) when delivered as a train of pulses.

The E-fields of the EC and MI methods differ in important ways¹⁰. First, for MI the E-field amplitude is linearly proportional to the frequency of the current source whereas the EC E-field amplitude is independent of this frequency. Second, the E-fields for the two methods exist in orthogonal

subspaces. While they can never be identical, they can in principle be spatially similar with respect to focality on the cortical surface. Third, for spatially similar cortical E-fields, the ratio of the EC-to-MI scalp E-field (root-mean-square) increases as cortical focality increases. For the focality of a typical TMS coil this ratio is estimated to be approximately 10 and reaches a limiting value of 18 as focality is increased. Thus, the scalp E-field amplitude ultimately places a severe constraint on the focality and amplitude of EC cortical E-fields. Estimates of the EC cortical E-fields in the physiological frequency range suggest that the maximum for most human participants is around 0.5 V/m^{11,12}; beyond this value scalp sensory stimulation becomes detectable and soon intolerable. MI systems are far less burdened by constraints imposed by the scalp E-field amplitude, allowing the method to be used to produce both subthreshold and suprathreshold cortical E-fields (as with TMS).

Another major difference between EC and MI methods arises due to energetic requirements. The generation of cortical E-fields in the endogenous frequency range of 0-200 Hz is very costly for MI methods. To obtain a 0.5 V/m cortical E-field amplitude at 10 Hz with tACS requires about 0.02 W/cycle delivered to the electrodes. To achieve the same E-field using a typical TMS coil would require approximately 600 kW/cycle delivered to the coil! However, the energetic cost of the MI method can be reduced to a manageable level by operating at higher frequencies. For example, to deliver a 0.5 V/m cortical E-field using a typical TMS coil at 2.0 kHz would require an average power of approximately 9 W/cycle, while a 2.0 V/m cortical E-field at 2.0 kHz would require less than 150 W/cycle.

An important application of NIBS is to modulate endogenous frequency activity. Due to the energetic costs of MI methods, the coupling between neurons and the NIBS E-field on the time scale of endogenous frequencies is achieved by other means. One means of introducing such timescales is through amplitude modulation. To this end, rTMS uses a waveform consisting of a kHz carrier frequency together with amplitude modulation (AM) and, to lesser extent, phase

modulation (PM) to achieve its effects. The carrier frequency of rTMS is a fixed value chosen by the manufacturer and is typically in the range of 3-4 kHz. The AM waveform is quite inflexible consisting of a sequence of boxcar-like functions that permit a damped single or half cycle of the kHz carrier frequency (a pulse) at programmable intervals. The phase-modulation is such that each TMS pulse begins at the same phase. These restrictions on the waveform are due to the TMS current source, a periodically charging and discharging capacitor which delivers a few thousand amperes to the TMS coil. The tACS current source, on the other hand, is a low-power and large-bandwidth amplifier which delivers a few milliamperes to the electrodes. As such, there are essentially no practical limitations with respect to the tES waveform.

To increase the experimental flexibility of NIBS methods and the robustness of its effects we have developed a new MI method, kilohertz transcranial magnetic perturbation (kTMP) (see Fig.1). The kTMP E-field is characterized by the waveform flexibility of tES along with the focality and potential amplitude range of TMS. The amplitude of our prototype kTMP system, as large as 8 V/m at 5 kHz, far exceeds that of tES. In contrast to capacitor-driven TMS, the kTMP current source is a high-current large-bandwidth amplifier often used to provide the magnetic field gradients of magnetic resonance imaging. As with the amplifier driven tES method there are almost no practical limitations with respect to the kTMP waveform. The experimenter may vary carrier frequency, AM, and PM over a wide range to investigate their NIBS effects. Multiple amplifiers driving the magnetic induction coil in a parallel can be used to obtain E-field amplitudes equal to those of TMS.

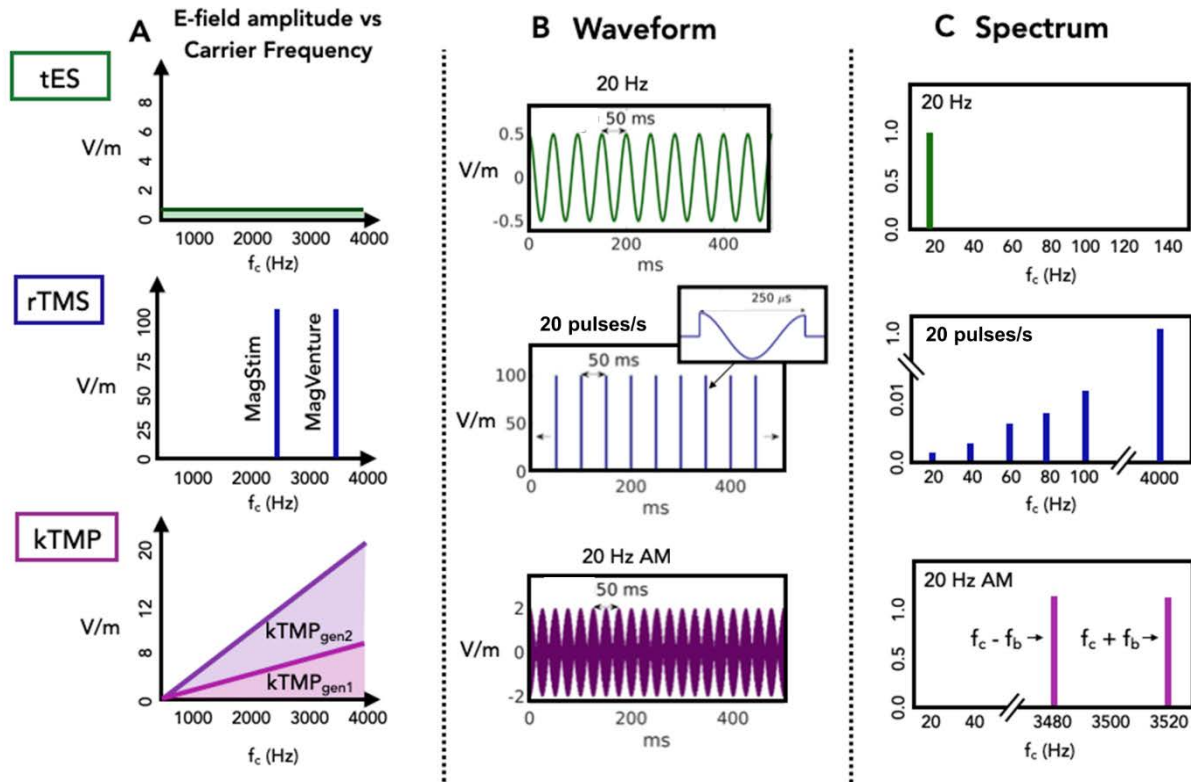


Fig. 1. E-field amplitude, carrier frequency, amplitude modulation and spectral differences between tES, rTMS and kTMP. The maximum E-field amplitudes for each method as a function of the carrier frequency f_c . The maximum E-field amplitude for EC methods is independent of the carrier frequency whereas the maximum amplitude of MI E-fields is linearly proportional to the carrier frequency f_c of the current source. The carrier frequencies for rTMS are fixed values set by the device manufacturer whereas the carrier frequencies of tES and kTMP are variable within the bandwidth specifications of the current source. A next generation kTMP system could provide E-field amplitudes equal to those of TMS. Column B: The amplitude modulated waveforms when targeting 20 Hz endogenous frequencies with tES at 20 Hz, rTMS at 20 pulse/s and kTMP at a 20 Hz beat frequency. The insert shows a single TMS pulse obtained by multiplying the carrier waveform by a boxcar-like (boxcar with slight exponential decay) amplitude-modulation function. The amplitude modulation waveforms for kTMP are very flexible. Here we depict the type of modulation used in this work, a sinusoid that produces a beating amplitude. Column C. Frequency spectra when targeting 20 Hz endogenous frequencies with tES at 20 Hz, rTMS at 20 pulse/s and kTMP at a 20 Hz beat frequency. The value plotted along the y-axis is a unitless ratio of the spectral amplitude at frequency f to the peak spectral amplitude. In rTMS the resultant frequency spectrum has infinite peaks at the harmonics of the rate of stimulation. Moreover, the harmonic of largest amplitude (not shown) is located at the reciprocal of the biphasic TMS pulse length (approx. 4 kHz) rather than at the targeted rTMS rate. With sinusoidal amplitude modulation at beat frequency f_b the kTMP spectrum has sideband peaks at $f_c - f_b$ and $f_c + f_b$.

Since neurons near resting membrane potential act as low-pass filters, a critical question centers on whether and by what mechanism narrow band kHz E-fields can effectively couple to the transmembrane potential to influence neural activity. We take up the mechanism question in the Discussion section. Here we note the impressive body of empirical results supporting a coupling

between kHz E-fields and neuronal dynamics, comprehensively reviewed in Neudorfer et al¹³. This work targets sub- and suprathreshold E-fields using in vitro models, as well as invasive and non-invasive in vivo studies with various species, including humans. To date, narrow-band kHz studies have used EC methods due to the absence of narrow-band MI devices. Subthreshold rTMS is spectrally peaked at its kHz carrier frequency. However, its spectrum has broad sidebands due to the brief boxcar function used for AM and contains peaks at all harmonics of the rTMS pulse rate. Thus rTMS, while widely employed to examine pulse rate-specific effects, is not appropriate for isolating frequency-specific effects at kHz frequencies.

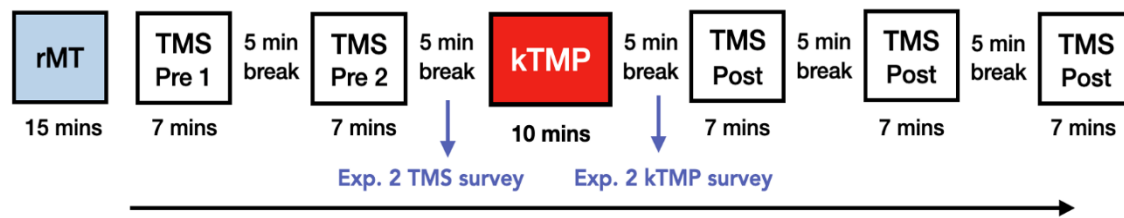
We report here the results of two experiments with human participants that evaluate the efficacy of kTMP in modulating cortical excitability. Adopting what has been the “gold standard” for evaluation the efficacy of NIBS methods^{14–17}, we used suprathreshold TMS, measuring motor evoked potentials (MEPs) elicited in a hand muscle, comparing the amplitude of the MEPs before and after kTMP stimulation. For both experiments the kTMP amplitude was set to produce a cortical E-field amplitude of approximately 2.0 V/m at the targeted primary motor cortex. In Experiment 1, we tested non-amplitude modulated kTMP at three different carrier frequencies (2 kHz, 3.5 kHz and 5 kHz), comparing these conditions to a sham condition (0.01 V/m at 3.5 kHz). In Experiment 2, we set the carrier frequency at 3.5 kHz and used AM to create beat frequencies of either 20 Hz or 140 Hz. In both experiments, we observed a robust increase in MEPs following kTMP stimulation, with the effect of a 3.5 kHz carrier frequency enhanced with amplitude modulation.

Results

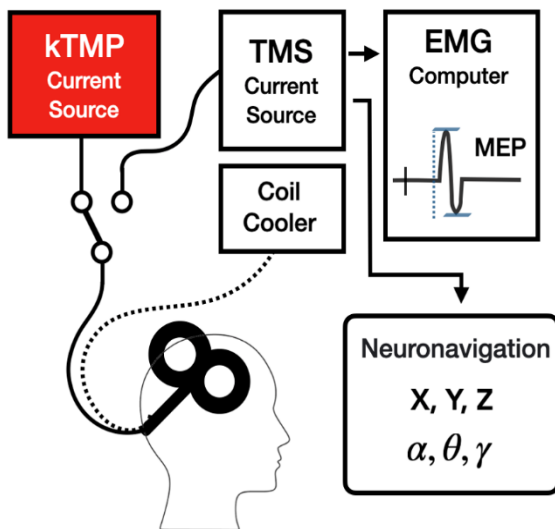
The experimental design is summarized in Fig. 2. We sandwiched five probe blocks around kTMP stimulation (active or sham). For the probe blocks, a commercial TMS unit was used to drive the

coil in the suprathreshold range to elicit MEPs. Each block included a single-pulse protocol and two paired-pulse protocols (short intracortical inhibition, SICI; intracortical facilitation, ICF). The two pre-stimulation blocks were used to establish baseline measures and assess reliability. Three post stimulation blocks were included to assess changes in neural excitability at three time points after kTMP stimulation.

A Experimental protocol



B Experimental hardware



C Experimental conditions

Exp1: Non-modulated kTMP

	SHAM	ACTIVE	ACTIVE	ACTIVE
Carrier	3.5 kHz	2 kHz	3.5 kHz	5 kHz
Beat	None	None	None	None
E-Field	0.01 V/m	2 V/m	2 V/m	2 V/m

Exp 2: AM-kTMP

	SHAM	ACTIVE	ACTIVE	ACTIVE
Carrier	3.5 kHz	3.5 kHz	3.5 kHz	3.5 kHz
Beat	None	None	140 Hz	20 Hz
E-Field	0.01 V/m	2 V/m	2 V/m	2 V/m

Fig. 2. Experimental setup and protocol. A) At the beginning of each session the rMT was determined at the hotspot (identified and marked during Session 1), followed by five TMS probe blocks, two that occurred prior to kTMP stimulation and three that followed kTMP stimulation. Each TMS block consisted of 90 suprathreshold TMS trials (30 single pulse, 30 SICI, 30 ICF), with each trial separated by a 4 - 5 s interval. In Exp 2, we administered a short survey to obtain subjective reports of sensory experience after the second TMS probe block and at the end of the kTMP stimulation. B) The experimental hardware consisted of the suprathreshold TMS current source, subthreshold kTMP current source, a figure-eight TMS coil, EMG system, and neuronavigation system. A switch allows the TMS coil to be driven by either the TMS or kTMP current source. C) Experimental conditions. In Exp 1, three carrier frequencies, set to produce a 2 V/m E-field at that surface of the motor cortex, were tested (each in a separate session), along with sham kTMP. In Exp 2, the non-modulated 3.5 kHz and sham conditions were repeated, along with two amplitude modulation conditions. In both experiments, kTMP stimulation was for 10 min.

After cleaning the MEP data (see Methods), there were a minimum of 20 MEP measures per protocol in each assessment block for each individual, a sufficient number for performing the MEP analyses^{18–21}. For each stimulation protocol, the average MEP amplitude was calculated for each block, and the effect of kTMP stimulation was operationalized as the percent change relative to the two baseline blocks (averaged across these blocks). This resulted in three post-kTMP measures per participant per condition (see Statistical Analysis for details). A value of 0% would indicate no change in MEP amplitude from pre- to post-stimulation, whereas a value of 100% would indicate the MEP amplitude doubled from pre- to post-stimulation.

Experiment 1: Non-Modulated kTMP

In the first experiment, we assessed the effect of 10 min of non-modulated kTMP stimulation with a cortical E-field amplitude of 2 V/m (see Methods, EQ 1), comparing three stimulation frequencies (2 kHz, 3.5 kHz and 5 kHz) to a sham kTMP condition (0.01 V/m, 3.5 kHz). We used a within-subject design, testing each participant in all four conditions (order randomized) with a minimum of two days between sessions. Five of the 19 participants only completed three of the four sessions conditions due to technical issues with theBrainsight Neuronavigation system ($n = 1$) or university suspension of testing with human participants in March 2020 due to the onset of the COVID-19 pandemic ($n = 4$). To account for missing data, we used a mixed-effects model with fixed factors of stimulation frequency and post-stimulation block, and a random factor of participant.

Single Pulse: We first assessed the reliability of our dependent measure, focusing on the single-pulse data from the two baseline blocks. The mean MEP amplitude was highly correlated across participants ($r = 0.93$, $p < .001$), with no difference between the two blocks (Difference = .037 mV, $t(70) = 1.048$, $p = .299$). This analysis indicates that this MEP measure was very reliable across the two timepoints tested prior to kTMP stimulation.

Turning to the main data of interest, Fig. 3 shows the percent change in MEP amplitude post-kTMP relative to pre-kTMP, with the data averaged across post-stimulation blocks (3A) and for each of the three post-stimulation blocks individually (3B). The effect of stimulation frequency was significant [$\chi^2(3) = 10.841, p < 0.05$]: Cortical excitability increased following non-modulated kTMP. There was no effect of post stimulation block [$\chi^2(2) = 1.433, p > 0.4$] nor was the interaction significant [$\chi^2(6) = 8.415, p > 0.2$]. Thus, in terms of the overall pattern, there was an increase in corticospinal excitability following kTMP stimulation and this effect persisted for at least 35 min.

To further evaluate the main effect of frequency, we compared the percent change for each active condition to sham. These comparisons revealed that MEPs increased after 3.5 kHz kTMP stimulation [$\chi^2(1) = 7.982, p < 0.01$] and after 2 kHz kTMP stimulation [$\chi^2(1) = 4.107, p < 0.05$] compared to sham. In contrast, there was no effect of 5 kHz stimulation [$\chi^2(1) = 3.186, p > 0.05$].

SICI: We first confirmed that MEPs to the suprathreshold TMS pulse were attenuated in the paired-pulse protocol when the subthreshold conditioning stimulus was presented 3 ms in advance of the test pulse. To this end, we computed the ratio of the paired-pulse MEP amplitude to that observed on single pulse trials. We restricted this analysis to the pre-stimulation data to avoid confounding with the effect of kTMP stimulation, pooling the data across the two pre-kTMP blocks and across all four sessions. This analysis showed a strong SICI effect, with a mean attenuation of 58% on the paired-pulse trials relative to the single pulse trials [$t(70) = -19.571, p < .001$; Fig. 3C]. A similar level of attenuation was observed in the post-kTMP blocks following sham stimulation.

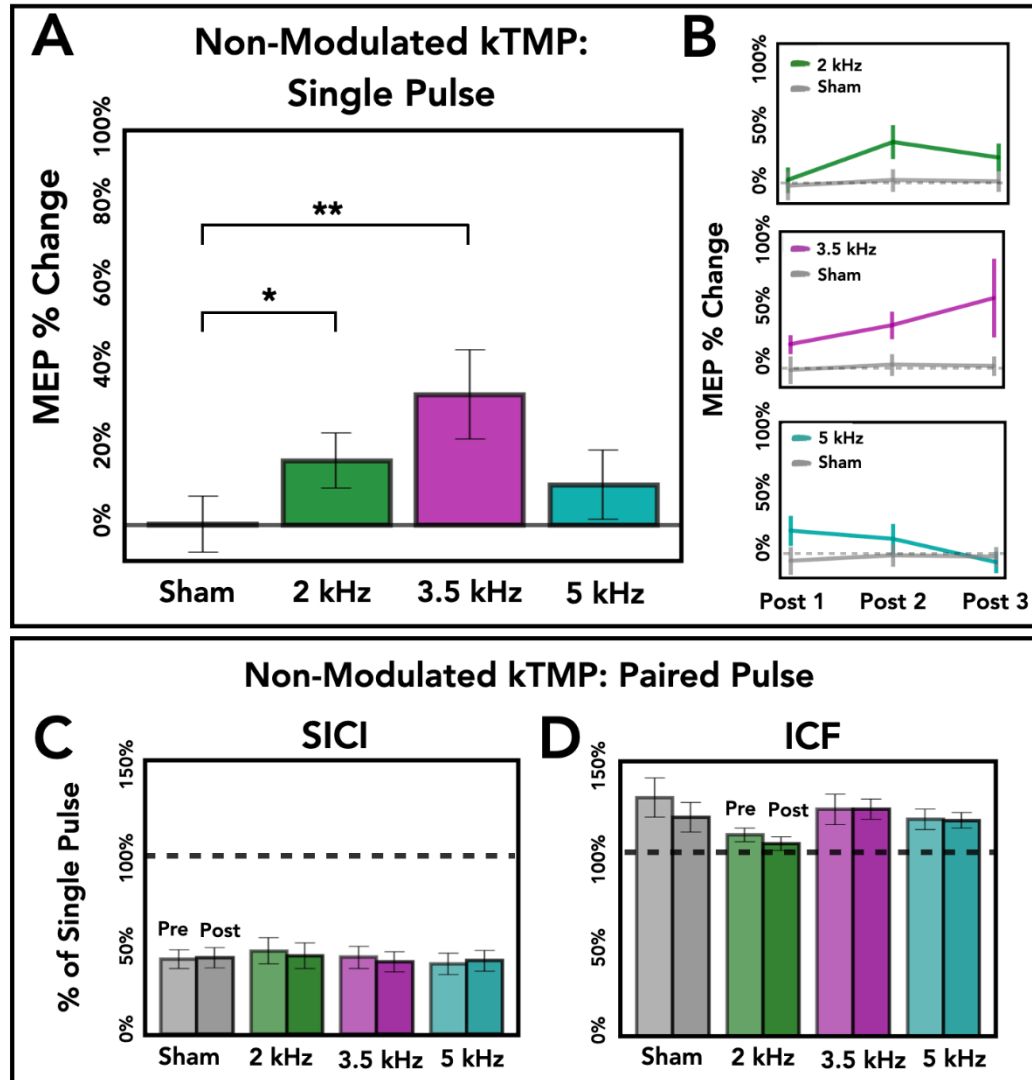


Fig. 3. Non-modulated kTMP increases cortical excitability. A) Change in MEP amplitude measured with single-pulse, suprathreshold TMS following kTMP stimulation, relative to baseline. Compared to sham, MEPs increased following 2 kHz and 3.5 kHz kTMP. B) Single-pulse MEP results plotted separately for the three TMS blocks administered after kTMP. The first block started approximately 5 min after kTMP and the other two started approximately 12 min after the preceding block. The effect of block was not significant, nor the block x condition interaction. C/D) Change in SICI and ICF measured with paired-pulse protocols, relative to baseline. While both of the expected paired-pulse effects were observed, neither SICI or ICF changed following kTMP stimulation.

We then asked if the magnitude of the SICI effect was modulated by active kTMP using the same mixed-effect model as in the single-pulse analysis. There was no effect of stimulation frequency [$\chi^2(3) = 1.016, p > 0.7$], no effect of post-stimulation block [$\chi^2(2) = 3.824, p > 0.1$] and no interaction between the two factors [$\chi^2(6) = 1.265, p = 0.974$]. Thus, kTMP does not appear to influence the magnitude of intracortical inhibition.

ICF: Similar to SICI, we first confirmed that MEPs to the suprathreshold test stimulus increased when the subthreshold conditioning stimulus was presented 10 ms in advance of the test pulse. MEP amplitude was greater in this paired-pulse condition compared to the single pulse protocol, with a mean effect of facilitation of 19% [$t(70) = 5.141$, $p < .001$; Fig. 3D]. However, as with SICI, there was no evidence that kTMP, as tested here, influenced ICF: There was no effect of stimulation frequency [$\chi^2(3) = 4.473$, $p > 0.2$], no effect of post-stimulation block [$\chi^2(2) = 1.332$, $p > 0.5$], and no interaction between the two factors [$\chi^2(6) = 2.009$, $p > 0.9$].

In summary, non-modulated kTMP at 2 kHz and 3.5 kHz produced an increase in corticospinal excitability as measured with single pulse TMS. Relative to sham, kTMP at 5 kHz did not produce a significant increase in corticospinal excitability, suggesting that the effect of kHz-induced E-fields may be frequency specific. However, this hypothesis must be treated cautiously given that there was no difference between the three active conditions when directly compared [all χ^2 's < 3.783 all p 's > 0.05]. Although our paired pulse SICI and ICF protocols exhibited the standard pattern of inhibition and facilitation, respectively, non-modulated kTMP did not impact these measures.

Experiment 2: Amplitude Modulated kTMP (AM-kTMP)

The main goal of the second experiment was to evaluate the effect of AM-kTMP on cortical excitability. To this end, a carrier frequency of 3.5 kHz was amplitude modulated (see Methods and fig. 1), to produce beat frequencies at 20 Hz or 140 Hz, frequencies chosen because of their relevance to endogenous activity in motor cortex²²⁻²⁴. The stimulation intensity was set to produce an E-field of 2 V/m at the cortical surface. As points of comparison, we also included a non-modulated 3.5 kHz condition (at 2 V/m) and a sham condition (3.5 kHz carrier with E-field set to 0.01 V/m). The inclusion of these two latter conditions also provides a replication of the most

prominent effect reported in Exp. 1. Thirteen of the 16 participants completed all four sessions. Three completed only three sessions, one due to a technical problem with the Brainsight system and two due to university suspension of NIBS testing during the pandemic.

Single Pulse: We first verified that the MEP measures remained stable during the two baseline blocks. Mean MEP amplitudes were positively correlated across the two blocks ($r = 0.83$, $p < .001$) and there was no significant difference between blocks [$\bar{X}_{\text{Diff}} = .057$, $t(60) = 1.671$, $p = .100$].

We next examined the non-modulated 3.5 kHz condition since this provides a replication of the condition in Exp1 that produced the most robust effect of kTMP. We again found that the 3.5 kHz condition significantly increased corticospinal excitability relative to sham [$\chi^2(1) = 11.032$, $p < 0.001$]. As can be seen in Fig. 4, the magnitude of the increase, as well as variability across participants was similar to that observed in Exp 1.

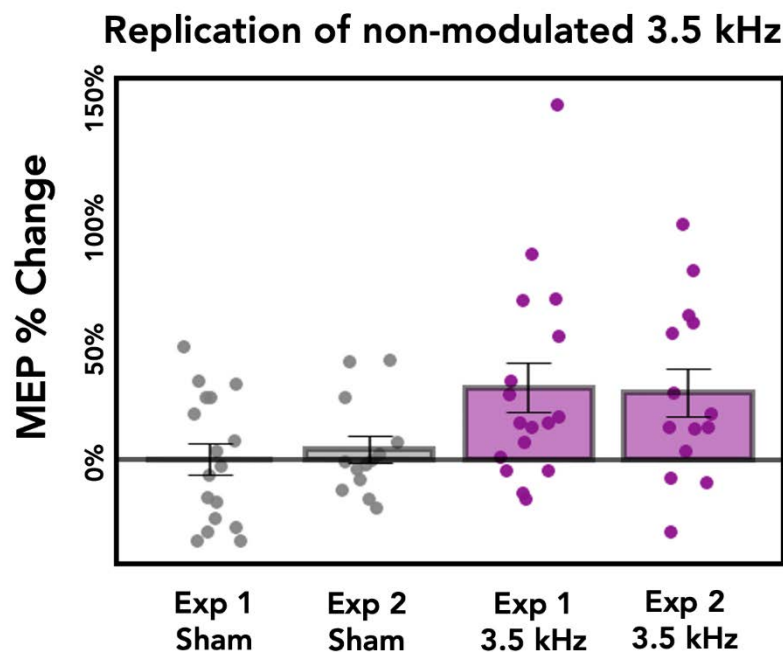


Fig. 4. Increase in cortical excitability following non-modulated 3.5 kHz kTMP replicates in Exp 2. Change in MEP amplitude measured with single-pulse TMS following kTMP stimulation, relative to baseline. For comparison, the data from Exp 1 are replotted alongside the data from Exp 2 for the 3.5 kHz and sham conditions. Each dot indicates the data from a single participant.

Fig. 5A shows the percent change in MEP amplitude post-kTMP relative to pre-kTMP for all four conditions. A mixed-effect model revealed a significant effect of stimulation frequency [$\chi^2(3) = 17.211, p < 0.001$], a significant effect of post-stimulation block [$\chi^2(2) = 6.255, p < 0.05$], with no interaction between the two factors [$\chi^2(6) = 2.402, p > 0.8$]. Planned comparisons showed

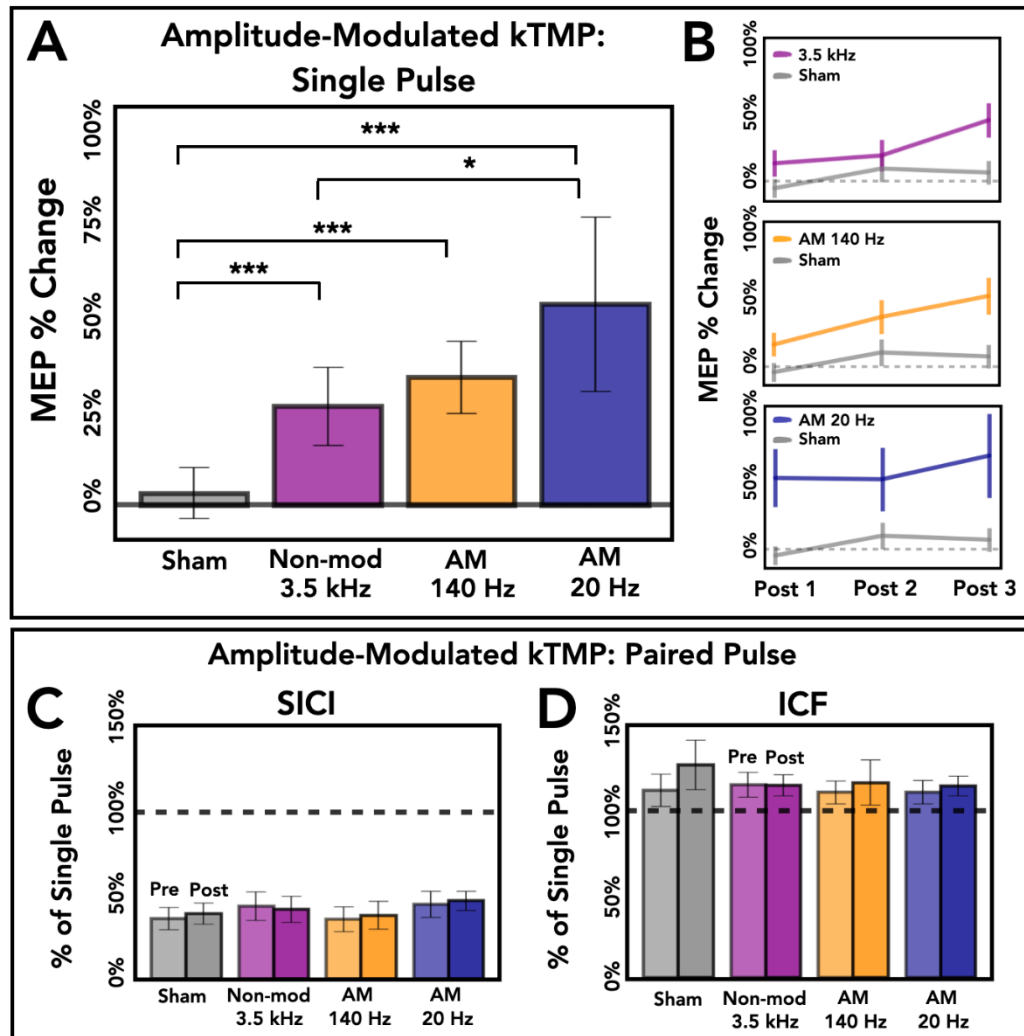


Fig. 5. Amplitude-Modulated kTMP. A) Single Pulse average percent change across conditions. Percent change in MEP amplitude from pre to post kTMP stimulation across the four experimental conditions. Compared to sham, an increase in MEP amplitude was found for all three of our experimental conditions compared to sham. In addition, AM-kTMP at 20 Hz increased MEPs significantly above that for non-modulated 3.5 kHz, suggesting AM kTMP stimulation at some AM frequencies may be more effective than non-modulated kTMP. B) Single Pulse time course post kTMP. Time course of MEP percent change across the three TMS blocks post kTMP stimulation. Time in-between each post TMS block is approximately 12 minutes. An effect of time post stimulation was found with non-modulated 3.5 kHz and AM 140 Hz increasing significantly across time; no effect of time was found for sham or AM 20 Hz. C) SICI protocol. We again saw a substantial inhibitory effect for the SICI protocol compared to single pulse, but AM-kTMP did not have an effect on the amount of inhibition elicited. D) ICF protocol. Same as C except for facilitatory protocol.

that MEPs increased significantly after AM-kTMP stimulation at 20 Hz [$\chi^2(1) = 13.816, p < 0.001$] and 140 Hz [$\chi^2(1) = 15.412, p < 0.001$] compared to sham. More important, MEP amplitude in the 20 Hz AM condition was significantly greater than non-modulated kTMP at 3.5 kHz [$\chi^2(1) = 6.503, p < 0.05$]. This comparison indicates that AM-kTMP at 20 Hz has a stronger effect on cortical excitability than non-modulated kTMP for an E-field of identical peak amplitude. There was also an increase in MEP amplitude in the 140 Hz condition compared to non-modulated kTMP, but this difference was not significant [$\chi^2(1) = 1.098, p > 0.2$].

In terms of the effect of time (Fig 5B), MEP amplitude increased across the three post-kTMP blocks for the non-modulated 3.5 kHz condition [$\chi^2(2) = 16.329, p < .001$] and 140 Hz AM [$\chi^2(2) = 8.763, p < 0.05$]. This effect was not observed for the sham condition [$\chi^2(2) = 3.758, p > 0.1$] nor the 20 Hz AM condition [$\chi^2(2) = 1.679, p = 0.432$]. The latter is especially noteworthy, suggesting that the increase in corticospinal excitability following 20 Hz AM-kTMP persisted for at least 35 min. The overall pattern of an increase in the efficacy of kTMP across the post-stimulation blocks was unexpected, a point we return to in the Discussion.

Paired-pulse protocols: The SICI and ICF protocols were effective, producing a decrease and increase, respectively, in MEP amplitude relative to the single pulse protocol [SICI: $t(60) = -16.576, p < .001$; ICF: $t(60) = 2.976, p = .004$; Fig. 5C-D]. As in Exp 1, kTMP stimulation did not produce a change on either measure. For SICI, there was no effect of stimulation frequency [$\chi^2(3) = 1.614, p > 0.7$], no effect of post-stimulation block [$\chi^2(2) = 0.503, p > 0.7$], and no interaction between the two factors [$\chi^2(6) = 5.028, p > 0.5$]. Similarly, for ICF, there was no effect of stimulation frequency [$\chi^2(3) = 4.053, p > 0.2$], no effect of block [$\chi^2(2) = 0.148, p > 0.9$], and no interaction [$\chi^2(6) = 5.627, p > 0.4$].

In summary, we replicated the finding that non-modulated 3.5 kHz kTMP produces an increase in corticospinal excitability. In addition, 3.5 kHz AM-kTMP with a beat frequency of 20 Hz produced an increase in excitability above that observed with 3.5 kHz non-modulated kTMP.

Subjective experience during kTMP stimulation

Informal observations from the participants in Exp 1 indicated that the coil did not produce any detectable tactile or auditory sensation. The amplifier does produce a sound, but one that was effectively masked by playing a louder, pre-recorded sound (3.5 kHz tone) in all conditions.

We conducted a more formal assessment of subjective experience in Exp 2, administering a short survey twice, once just before and once just after kTMP stimulation (Fig. 2A). The former provides reports concerning the participants' experience of the TMS probes since it follows right after the second baseline block; the latter would assess the participants' experience of kTMP stimulation. Participants provided three ratings using an 11-point scale (0 = not at all; 10 = extremely) in response to questions on annoyance, pain, and muscle twitching.

Table 1 presents the means for each measure following TMS, active kTMP, and sham kTMP. In line with expectations for TMS²⁵, the participants were aware of occasional twitches in the finger, but the stimulation was well-tolerated in terms of annoyance and pain given that the coil was positioned over M1. Of primary interest for the present report, the modal rating was 0 for all three ratings following active kTMP. Given the low mean values and limited range, we did not do a statistical comparison of active and sham kTMP.

After completing the three ratings, participants were given an open-ended question to describe their subjective experience. Similar to previous reports²⁵, the comments following suprathreshold TMS stimulation noted involuntary hand movement (5 reports), face twitching (2 reports), a flicking sensation on the head (presumably the TMS tactile artifact, 8 reports), and a clicking noise (1

report). Only two comments were made following kTMP: One participant reported experiencing a headache following 20 Hz AM-kTMP. Another participant reported experiencing tingling in the fingers as if “my limbs were asleep” following 140 Hz AM-kTMP. In summary, while this is only a preliminary examination of the feelings and sensations experienced during active kTMP, the survey data and subjective reports suggest that kTMP is amenable to double-blind experimentation.

Stimulation method	Annoyance	Pain	Muscle Twitch
TMS	1.5 (1.4)	0.5 (0.7)	5.3 (1.6)
Active kTMP	0.5 (1.1)	0.1 (0.4)	0.2 (0.6)
Sham kTMP	0.1 (0.3)	0.0 (--)	0.4 (1.4)

Table 1. Mean ratings (SD in parenthesis) from Exp 2 on an 11-point scale in response to questions assessing annoyance, pain, and awareness of muscle twitching following second baseline TMS block or after kTMP stimulation.

Discussion

kTMP offers a novel method for exploring subthreshold NIBS experimental space. It combines the waveform flexibility of tES methods with the wider E-field range of TMS methods and, by using a TMS coil to deliver stimulation, retains the focality of TMS. Moreover, amplitude modulation of the flexible kTMP waveform allows us to mimic E-fields at frequency bands that correspond to those of well-documented endogenous neural rhythms (e.g., alpha, beta).

We conducted two experiments to assess the efficacy of kTMP in modulating neural activity, measuring MEPs before and after non-modulated kTMP and AM-kTMP. In Experiment 1 non-modulated kTMP with a targeted cortical E-field of 2 V/m in all conditions produced an increase in corticospinal excitability, a directional change similar to that observed with other methods using

subthreshold kilohertz stimulation¹³. Although we did not observe significant differences between the three carrier frequencies, the effect was most pronounced in the condition in which the carrier frequency was set to 3.5 kHz.

In Experiment 2 we replicated our finding that non-modulated kTMP at 3.5 kHz increases corticospinal excitability. We also observed increased corticospinal excitability for the two AM-kTMP conditions (20 Hz and 140 Hz, with a carrier frequency at 3.5 kHz) relative to sham. Critically, 20 Hz AM-kTMP produced an increase above that observed with non-modulated 3.5 kHz kTMP, suggesting that amplitude modulation at physiologically-relevant frequencies induces an additional change in excitability over that arising from stimulation in the kHz carrier frequency range.

The effects of kTMP were only observed with the single-pulse TMS protocol; we did not observe any effect of kTMP on the two paired-pulse protocols. The mechanisms through which these protocols probe corticospinal excitability are complicated. Both the orientation of the coil and targeted region of the cortex impact the manner in which the suprathreshold TMS pulse elicits MEPs: It can come about via direct excitation of the axons of the corticospinal neurons (D-wave) or via its effects on neurons that provide synaptic input to corticospinal neurons (I-wave). Given that the efficacy of kTMP was only observed with the single pulse probe using the standard M1 stimulation protocol (coil oriented along the anterior-posterior axis), we postulate that kTMP impacts the mechanisms that influence the early I-wave (for a review on circuits involved in NIBS see²⁶). We note, though, that this hypothesis is *post-hoc* and rests on a null result—the absence of an effect for the paired-pulse procedures. Moreover, prior studies using a combination of single- and paired-pulse procedures have yielded an inconsistent picture. For example, whereas single-pulse probes of NIBS efficacy generally produce consistent results (e.g., iTBS produce an increase in excitability; cTBS produces a decrease), the results from paired-pulse protocols are quite variable^{14,27,28}. The present results are encouraging in that, across a range of conditions, we

consistently observed an increase in cortical excitability in response to single-pulse TMS following the application of a 2 V/m E-field for 10 min.

More generally, we can speculate about the mechanisms by which kHz stimulation modulates neural state, both in terms of how the E-field is coupled to neurons and, once coupled, the resultant effects at the cellular and network level. As a starting point, we note that if neurons behave as low-pass filters (as is commonly assumed), kHz E-fields, even if amplitude modulated could not modulate neural excitability. However, the low pass filtering assumption is rooted in the treatment of neurons as linear, time-invariant systems near resting membrane potential. If the transmembrane potential departs significantly from the resting value, then the neuron must be modeled as an active electrical system which, by virtue of voltage-dependent membrane resistance, requires nonlinear models (e.g., Hodgkin and Huxley, 1952). Furthermore, neurons need not pass kHz frequency components to have an effect upon the transmembrane potential.

We suggest three mechanisms by which kHz E-fields may couple to the neuron transmembrane potential. First, high frequency signals could be passed during short intervals. As the membrane potential nears threshold (due to synaptic input) the sodium ion membrane conductance can increase by two orders of magnitude²⁹. This will effectively decrease the membrane time constant (the product of membrane resistance and capacitance) and increase the cutoff frequency by the same factor. For example, the cutoff frequency for the resting membrane of pyramidal cells is approximately 20 Hz³⁰; when near threshold the cutoff frequency could transiently increase to approximately 2 kHz, providing a possible mechanism for the effects of non-modulated kTMP.

Second, coupling may come about from demodulation whereby the envelope of a kHz presynaptic transmembrane potential may be passed to a postsynaptic cell. An AM signal can be demodulated to produce the component frequencies of its modulation envelope through sequential rectification and low-pass filtering. Gap junctions in some electrical synapses of the mammalian brain operate as current rectifiers (see review, Faber and Pereda, 2018). Therefore, an AM kHz signal passed

to a near-threshold transmembrane potential of a presynaptic neuron may appear as a demodulated signal in a near-rest post-synaptic neuron acting as a low-pass filtering.

Third, coupling might come about from intermodulation. Intermodulation is a process exhibited by nonlinear systems whereby input frequencies f_1 and f_2 can produce output frequencies at $nf_1 - mf_2$ (where n, m are integers). Thus, when the AM signal is created by the superposition of two kHz signals (as with AM-kTMP), intermodulation can produce frequencies in the endogenous frequency range (0-200 Hz)^{32,33}.

Future studies will need to address the mechanisms responsible for kTMP and its impact on cortical excitability. We note that the magnitude of the increase in cortical excitability in both experiments is similar to that observed in the initial reports of tES and rTMS protocols that used a single-pulse TMS protocol to assess efficacy^{15,34,35}. While this is surprising given the striking differences between the methods, it is also difficult to make comparisons given the effect of NIBS is likely dependent on not just the amplitude but also the direction, frequency, and duration of the applied E-field. The interplay of these factors may account for the fact that efforts to establish dose-dependent response functions with NIBS protocols have provided very mixed results^{36,37}. A limiting factor for tES studies of dose-dependency is that these methods are restricted to the very low end of subthreshold space in terms of E-field amplitude. In contrast, kTMP opens up a large subthreshold experimental space, one in which there is considerable range in terms of E-field amplitude, carrier frequency, AM waveform, and stimulation duration. Not only should the broad kTMP space be well-suited for studying dose-dependency, but we may find regimes within this space in which kTMP produces an inhibitory effect on neural excitability.

At present, we have sampled just a small part of this space given that we set the E-field to 2 V/m in both experiments and limited kTMP stimulation to 10 min. While the theoretical upper boundary for our current system is 8 V/m (at 5 kHz), this range can be easily expanded by using a more powerful amplifier or running multiple amplifiers in parallel. Our calculations indicate that safety

issues will remain negligible up to 15 V/m at 10 min. Higher E-fields and/or longer durations (at these higher E-fields) will require empirical evaluation involving bench tests and possibly animal models.

On the evaluation side, we have only assessed the impact of kTMP on neural excitability out to 35 min post-stimulation. A priori, we made this decision given a desire to limit the experimental session to two hours and expected that an effect, if observed would start to dissipate in the last block. Surprisingly, the pattern in both experiments suggests that the effect of kTMP may become more pronounced over the 30-min window. Extending the duration of the post-stimulation probe is another priority for future testing.

In addition to offering a large subthreshold experimental space, there are a number of other noteworthy features of kTMP. First, kTMP is ideally suited for double-blind experimentation. As verified in the subjective reports of our participants, the only percept associated with 2.0 V/m kTMP is a tone at the carrier frequency emanating from the amplifier, one that can be easily masked. Even when positioned over the prefrontal or occipital cortex, there is no peripheral nerve stimulation or tactile percept from kTMP stimulation, issues that can impact TMS and tES protocols.

Second, for studies using TMS as a probe on NIBS efficacy, the E-fields of the perturbation (e.g., kTMP) and probe (e.g., suprathreshold single-pulse TMS) are matched up to a scale factor. In contrast, the E-fields of tES and TMS cannot be matched¹⁰ and, as such, likely impact different neural populations even when the targeted region is ostensibly the same. Beyond the experimental convenience of using the same TMS coil for both perturbation and probe as in our prototype, the E-field alignment may increase experimental robustness.

Third and perhaps most exciting are the manipulations made possible with AM-kTMP given that this approach combines an expanded range of subthreshold E-field amplitudes with AM waveform and carrier frequency flexibility. Future work is required to determine the AM and carrier frequency

(and location) specificity of these effects, something that has been explored with considerable success in the tACS and rTMS literatures. Importantly, the experimenter can create a kTMP waveform of unlimited complexity and flexibility, with the resulting stimulation pattern completely specified in terms of its E-field spectrum. We foresee no serious technical problems in running concurrent kTMP-EEG experiments given that the artifact from the kHz carrier frequency can be easily filtered out. This approach will make it possible to measure entrainment effects between the exogenous kTMP waveform and endogenous brain rhythms. Moreover, this approach can be used to tailor the stimulation waveform on an individual basis or for closed-loop control, promising avenues for translational applications of NIBS.

The expanded E-field range of kTMP also makes this approach ideal for tailoring the level of stimulation on an individual basis. Similar to many TMS studies, individual thresholds can be determined with single pulse TMS, and the threshold can then be used to adjust the intensity of the kTMP stimulation as a way to roughly equate “effective stimulation”. In this way, one can empirically modify the stimulation level to account for factors such as skull thickness, skull-to-cortex distance, and cortical morphology known to influence the amplitude of the cortical E-field^{38,39}. While the frequency of stimulation with tACS can be tailored on an individual basis, the limited E-field range of EC methods makes it impractical to vary the intensity of stimulation between individuals.

Conclusion

NIBS has provided a powerful approach for safely perturbing brain activity, one that has been employed in basic research to test functional hypotheses concerning brain-behavior relationships spanning all aspects of human cognition with increasing translational applications. kTMP offers an opportunity to explore a new experimental space, one with a relatively large range of

subthreshold E-field induction, the focality of TMS, and the ability of imposing E-fields at physiological relevant frequencies.

Methods

Apparatus

Kilohertz Magnetic Perturbation (kTMP) system

The kTMP system consists of a high-amplitude current source, a TMS coil, and a control system. The same TMS coil may be connected to either the kTMP current source or to a commercial TMS power supply system (MagVenture MagPro x100 TMS stimulator), permitting interleaved kTMP-TMS experiments and ensuring identical kTMP and TMS E-field distributions up to an amplitude scaling factor. The kTMP amplifier (AE Techron Model 7794) is a voltage-controlled current source capable of delivering up to 200 A to the coil. We used a passive liquid-cooled figure-8 coil (MagVenture Cool-B65; i.d. 35 mm, o.d. 75 mm).

The kTMP control system consists of a personal computer (PC), input/output PCI card, and a custom interface to read the coil's built-in temperature sensor. Using a data acquisition toolbox (Mathworks R2018a), the PCI card was programmed to deliver analog input to the amplifier, thus specifying the temporal waveform of the E-field. The input waveform can be either a fixed sinusoidal frequency or the waveform can be amplitude modulated.

Bench testing indicated that the system when running in kTMP mode did not produce marked changes in coil temperature. As an added safeguard, the PCI card was set up to receive an analog input from the coil's temperature sensor and create an automatic shutdown if the coil temperature exceeded 48°C, following guidelines established by the International Electrotechnical Commission (IEC). In practice, for E-fields up to the 2 V/m limit used in the present experiments, the coil temperature never rose above 32° C during system operation.

Participants

29 young adults were recruited through various advertisements posted to the UC Berkeley and Berkeley communities. 19 were tested in Experiment 1 (12 female, 7 male) and 16 were tested in Experiment 2 (10 female, 6 male, seven of whom had been tested in Exp 1). All participants were naive to the purpose of the study, provided informed consent, and were financially compensated. Given the novelty of kTMP as a NIBS method, the IRB at UC Berkeley enlisted an outside expert and members of the campus Environmental and Health Safety Committee to evaluate the system. Following their reports, the protocol was approved by the IRB at UC Berkeley with the kTMP system deemed a non-significant risk device for e-fields up to 8 V/m.

Procedure

Overview

To evaluate the kTMP system as a new tool to modulate neuronal excitability, we measured the impact of kTMP on corticospinal excitability using suprathreshold TMS stimulation over motor cortex. Figure 2 depicts an overview of the experimental hardware and protocol. In brief, kTMP stimulation was sandwiched by five 7-min probe blocks, each of which consisted of a trio of TMS assays of cortical excitability. Two of the probe blocks occurred prior to kTMP and three occurred after kTMP.

Each experiment consisted of five 2-hr test sessions, with each session separated by a minimum of 2 days. The first test session was used to determine the optimal coil position (“hotspot”) and threshold intensity for eliciting MEPs with suprathreshold single-pulse TMS (see below). The position of the hotspot was recorded by a neuronavigation system (BrainSight). This allowed the experimenter to return to the same position for each TMS block (see below), as well as during the application of kTMP. The other four test sessions were used to test the efficacy of different kTMP

parameters on cortical excitability with a focus on variation of the carrier frequency for non-modulated kTMP in Exp 1 and amplitude-modulated kTMP in Exp 2 (Fig. 2C). Two steps were taken to create a double-blinding protocol. First, we created a coding system such that the experimenter typed in a number that was paired to the desired stimulation condition in an arbitrary and random manner, one that varied across participants in a manner unknown to the experimenter. Second, we recorded the sound emanating from the amplifier when producing a non-modulated 3.5 kHz waveform and played this recording at a higher intensity as background sound during kTMP stimulation. This effectively masked the amplifier sound.

kTMP

For each carrier frequency, the current amplitude was selected to achieve a peak 2.0 V/m E-field at a distance of 14 mm perpendicular to the coil surface, a distance we took to represent the depth of the motor cortex from the overlying scalp⁴⁰. The method of Nieminen⁴¹ was used to measure the effective E-field amplitude in a spherical phantom as a standard. The relationship between the current amplitude I (amperes), carrier frequency f_c (Hz), and E-field magnitude E (V/m) at 14 mm was established to be:

$$E = (7.875 \times 10^{-6} \text{ Vs/Am}) f_c I \quad (\text{EQ. 1})$$

where V, s, A, and m, correspond to volts, seconds, amperes, and meters, respectively. As a function of time t , the AM-kTMP waveform is obtained by multiplying the carrier waveform by $\cos(2\pi f_b t)$ where f_b is the beat frequency (modulation frequency). Spectrally the beating AM signal would be composed of two peaks at frequencies f_1 and f_2 such that $f_b = (f_2 - f_1)/2$ (fig. 1).

Experiment 1. Non-modulated kTMP

We used a within-subject design, testing each participant between sessions on each of four kTMP stimulation conditions, with the order counter-balanced across participants. For three of the conditions, the carrier frequency (2 kHz, 3.5 kHz, 5 kHz) was paired with an intensity to create an E-field at the superficial aspect of the hand area of the motor cortex of 2 V/m. Note that we did not adjust for individual differences in scalp-to-cortex distance. For the sham condition, we used a 3.5 kHz carrier frequency producing a 0.01 V/m E-field at the cortical surface.

Experiment 2. Amplitude-modulated kTMP

We again used a within-subject design, testing each participant in four sessions. Two of the conditions were repeated from Exp 1: the 3.5 kHz unmodulated kTMP at 2 V/m and the sham condition. For the other two conditions, the carrier frequency was set at 3.5 kHz and the waveform was amplitude modulated to create beat frequencies of 20 Hz and 140 Hz. The 3.5 kHz carrier frequency was chosen since we had obtained the strongest effect at this frequency in Exp 1. We selected the 20 Hz beat frequency given the relevance of beta to motor function⁴²⁻⁴⁴ and the 140 Hz beat frequency based on literature concerning ripple effects at this frequency^{35,45,46}. The peak cortical E-field amplitude for the AM conditions was 2 V/m, identical to the non-modulated condition. Note that the inclusion of the 3.5 kHz non-modulated condition not only provides a replication of one condition in Exp 1, but also serves as the main point of comparison for the two AM-kTMP conditions.

TMS

Hotspot and Threshold Procedure (Session 1)

Single-pulse TMS was applied over left hemisphere M1 to determine the resting motor threshold (rMT) for the first dorsal interosseous muscle (FDI) in the right hand. We focused on FDI since it is relatively easy to isolate in all individuals and threshold values are very stable across test sessions ^{e.g., 47–49}.

The TMS coil was placed tangentially on the scalp with the handle pointing backward and laterally at 45° from the midline. The stimulator intensity was initially set to 30% of maximal stimulator output (MSO) and single pulses were generated at random intervals, with the experimenter visually monitoring the electromyography (EMG) output for MEPs. If no MEPs were detected after 2 or 3 pulses, the experimenter moved the coil a few mm. If a search over the candidate area failed to produce any MEPs, the stimulator output was increased (step size of 3%), with the location search repeated. Once MEPs were detected, a more focal search was conducted to identify the optimal location for eliciting MEPs. This location was registered in three-dimensional space using a neuro-navigation system (Brainsight, Rogue Resolutions Ltd., Cardiff, UK) to ensure consistent coil position during and between experimental sessions. rMT was defined as the minimum TMS intensity required to evoke MEPs of at least 50 μ V peak-to-peak amplitude on 5 of 10 consecutive trials. Trials in which background EMG was elevated were excluded.

The mean threshold was 58% (SD=11.3) and 63% (SD=11.1) of maximum stimulator output in Experiments 1 and 2, respectively. We repeated the threshold procedure in each of the kTMP sessions to capture possible intra-individual baseline changes in the cortico-excitability of the participants. In practice, the individual's threshold values remained very stable across days (mean deviation of 2.6%).

TMS Assays of Corticospinal Excitability (Sessions 2-5)

Each of the five probe blocks (two pre-kTMP and three post-kTMP) included single-pulse TMS (SP), and two paired-pulse protocols: short intracortical inhibition (SICI) and intracortical facilitation (ICF). These three protocols have been widely used in prior studies designed to evaluate the efficacy of tES and rTMS methods in altering neural excitability^{18,27,50}. For SP, the stimulation level was set at 120% of rMT. For the paired-pulse assays, the suprathreshold pulse was preceded by a sub-threshold conditioning stimulus set at 80% of rMT, with an interstimulus interval (ISI) of 3 ms or 10 ms for SICI and ICF, respectively. The probe block consisted of 90 trials, 30 for each of the three assays, with the order randomized within the block.

We developed a system to read and record the six-dimensional spatial and angular position of the coil with respect to the hotspot in real time. This information was recorded at the time of each TMS pulse and used to exclude trials in which the coil was distant from the hotspot or the angle had changed from the optimal hotspot orientation.

EMG

EMG activity was measured with a Bagnoli-8 EMG System (Delsys Inc.). EMG activity was recorded from surface electrodes placed over the right FDI muscles, with a reference electrode over the right elbow. The experimenter visually inspected the EMG traces on a monitor to ensure that the participant remained relaxed (i.e., negligible EMG background activity in FDI) and to detect the presence or absence of MEPs in response to the TMS pulses.

The EMG signals were amplified and bandpass filtered on-line between 20 and 450 Hz. The signals were digitized at 2000 Hz for off-line analysis. All EMG measures were analyzed with custom scripts written in Matlab 2018a. EMG was recorded continuously during the experiment.

The records were aligned offline with the TMS pulses based on a TTL pulse from the TMS system that was recorded by the EMG amplifier on an auxiliary channel.

Subjective Reports

We informally assessed the participants' subjective experience in Exp 1, focusing on reports concerning the perception of amplifier sound, tactile sensation, and discomfort. We formalized the process in Exp 2, administering a short survey concerning annoyance, pain and muscle twitching²⁵ after the second TMS probe block and at the end of the kTMP stimulation. The first survey was designed to obtain ratings on the subjective experience of suprathreshold TMS; the second was to obtain ratings on kTMP stimulation.

Data analysis

MEP. For each trial, the peak-to-peak amplitude of the MEP was calculated based on an epoch after the TMS pulse (15 to 50 ms after TMS pulse). Trials were excluded from the analysis based on the following criteria: 1) If the MEP amplitude was two standard deviations above or below the mean, with the mean and standard deviation calculated separately for each TMS assay (SP, ICF, ICI) for each probe block. 2) If the MEP amplitude was below .05 mV. 3) If the Brainsight recording indicated that the coil was more than 3 mm (Euclidian distance) from the optimal hotspot location or had an angular or twist error more than 5° from the optimal trajectory angle. 4) If noise in the EMG signal (200 ms - 50 ms) before the TMS pulse exceeded two standard deviations of the mean EMG signal. On average 10% (SD = 3%) of the trials were excluded per participant with a range of 4.8% to 20%.

The average MEP amplitude was calculated for each of the three TMS protocols in each probe block on an individual basis. SICI and ICF values were calculated by computing a ratio of the paired-pulse MEP average over the single pulse MEP average for each block.

We normalized the data for the post-kTMP blocks by calculating the percent change from the two baseline blocks (averaged together). This normalization was done separately for each probe block. Thus, the main analysis focuses on the three post-kTMP stimulation probe blocks for each of the three TMS assays (SP, SICI, ICF). We used a mixed-effects model with fixed factors of stimulation type (Exp1: 2 kHz, 3.5 kHz, 5 kHz, Sham; Exp 2: 3.5 kHz non-modulated, 20 Hz AM, 140 Hz AM, Sham) and post-stimulation block and a random factor of participant. This model was selected since it can accommodate missing data and subject variability. In addition, each active kTMP stimulation condition was tested against the sham condition and in Exp 2, we compared the two AM kTMP conditions to the 3.5 kHz non-modulated condition.

Acknowledgements

We are grateful to our team of undergraduate research assistants, Tatianna Howard, Alice Wang, Serena Chi, Caroline Cao, Lauren Anne Schuck, Emily Schultz, and Connor Brown, and Assaf Breska for his advice on the statistical analyses. We thank Angel Peterchev for his guidance throughout the development of this project. This work was supported by grants from the NIH (R21 EB028075; R35 NS116883) and NSF (EAGER 1946316). We thank MagVenture for providing the TMS stimulator and coil used in this study.

Author contributions

D.S., L.L., R.B.I. and B.I. conceived the project. D.S. designed and developed kTMP. L.L. designed the TMS experiments. L.L. and C.M. contributed to the collection of the data. C.M.

analyzed the data. L.L., C.M. and R.B.I. interpreted the TMS data. L.L., D.S., and C.M. drafted the paper, and all authors participated in the editing process. All authors approve the final version of the manuscript and are accountable for all aspects of the work. All persons designated as authors qualify for authorship, and all those who qualify for authorship are listed.

Conflict of Interest

The authors declare the following competing interests: LL, CM, BI, RBI and DS have stock ownership in Magnetic Tides, a non-publicly traded company created to develop new methods of non-invasive brain stimulation. UC Berkley holds the patent rights related to the kTMP technology but has provided Magnetic Tides with an exclusive licensing agreement.

Data availability

The data used to support the results are available upon request from the corresponding author.

References

1. Polanía, R., Nitsche, M. A. & Ruff, C. C. Studying and modifying brain function with non-invasive brain stimulation. *Nat. Neurosci.* **21**, 174–187 (2018).
2. Di Lazzaro, V. *et al.* Diagnostic contribution and therapeutic perspectives of transcranial magnetic stimulation in dementia. *Clin Neurophysiol* **132**, 2568–2607 (2021).
3. Fitzgerald, P. B. An update on the clinical use of repetitive transcranial magnetic stimulation in the treatment of depression. *J Affect Disord* **276**, 90–103 (2020).
4. Grigoras, I.-F. & Stagg, C. J. Recent advances in the role of excitation-inhibition balance in motor recovery post-stroke. *Fac Rev* **10**, 58 (2021).
5. Iglesias, A. H. Transcranial Magnetic Stimulation as Treatment in Multiple Neurologic Conditions. *Curr Neurol Neurosci Rep* **20**, 1 (2020).
6. Lefaucheur, J.-P. *et al.* Evidence-based guidelines on the therapeutic use of repetitive transcranial magnetic stimulation (rTMS): An update (2014-2018). *Clin Neurophysiol* **131**, 474–528 (2020).
7. Maatoug, R. *et al.* Non-invasive and invasive brain stimulation in alcohol use disorders: A critical review of selected human evidence and methodological considerations to guide future research. *Compr Psychiatry* **109**, 152257 (2021).
8. Huang, Y.-Z. *et al.* Plasticity induced by non-invasive transcranial brain stimulation: A position paper. *Clin Neurophysiol* **128**, 2318–2329 (2017).
9. Liu, A. *et al.* Immediate neurophysiological effects of transcranial electrical stimulation. *Nature Communications* **9**, 5092 (2018).
10. Sheltraw, D., Inglis, B., Labruna, L. & Ivry, R. Comparing the electric fields of Transcranial electric and magnetic perturbation. *J Neural Eng* (2021) doi:10.1088/1741-2552/abebee.
11. Huang, Y. *et al.* Correction: Measurements and models of electric fields in their vivohuman brain during transcranial electric stimulation. *Elife* **7**, (2018).

12. Vöröslakos, M. *et al.* Direct effects of transcranial electric stimulation on brain circuits in rats and humans. *Nat Commun* **9**, 483 (2018).
13. Neudorfer, C. *et al.* Kilohertz-frequency stimulation of the nervous system: a review of underlying mechanisms. *Brain Stimulation: Basic, Translational, and Clinical Research in Neuromodulation* **0**, (2021).
14. Huang, Y.-Z., Edwards, M. J., Rounis, E., Bhatia, K. P. & Rothwell, J. C. Theta burst stimulation of the human motor cortex. *Neuron* **45**, 201–206 (2005).
15. Nitsche, M. A. *et al.* Modulating parameters of excitability during and after transcranial direct current stimulation of the human motor cortex. *J. Physiol. (Lond.)* **568**, 291–303 (2005).
16. Nitsche, M. A. & Paulus, W. Sustained excitability elevations induced by transcranial DC motor cortex stimulation in humans. *Neurology* **57**, 1899–1901 (2001).
17. Nitsche, M. A. & Paulus, W. Excitability changes induced in the human motor cortex by weak transcranial direct current stimulation. *J. Physiol. (Lond.)* **527 Pt 3**, 633–639 (2000).
18. Chung, S. W., Hill, A. T., Rogasch, N. C., Hoy, K. E. & Fitzgerald, P. B. Use of theta-burst stimulation in changing excitability of motor cortex: A systematic review and meta-analysis. *Neurosci Biobehav Rev* **63**, 43–64 (2016).
19. Goldsworthy, M. R., Hordacre, B. & Ridding, M. C. Minimum number of trials required for within- and between-session reliability of TMS measures of corticospinal excitability. *Neuroscience* **320**, 205–209 (2016).
20. Cavaleri, R., Schabrun, S. M. & Chipchase, L. S. The number of stimuli required to reliably assess corticomotor excitability and primary motor cortical representations using transcranial magnetic stimulation (TMS): a systematic review and meta-analysis. *Syst Rev* **6**, 48 (2017).
21. Biabani, M., Farrell, M., Zoghi, M., Egan, G. & Jaberzadeh, S. The minimal number of TMS trials required for the reliable assessment of corticospinal excitability, short interval intracortical inhibition, and intracortical facilitation. *Neuroscience Letters* **674**, 94–100 (2018).

22. Feurra, M. *et al.* State-Dependent Effects of Transcranial Oscillatory Currents on the Motor System during Action Observation. *Scientific Reports* **9**, 12858 (2019).
23. Nakazono, H., Ogata, K., Kuroda, T. & Tobimatsu, S. Phase and Frequency-Dependent Effects of Transcranial Alternating Current Stimulation on Motor Cortical Excitability. *PLoS ONE* **11**, e0162521 (2016).
24. Wischniewski, M., Schutter, D. J. L. G. & Nitsche, M. A. Effects of beta-tACS on corticospinal excitability: A meta-analysis. *Brain Stimulation* **12**, 1381–1389 (2019).
25. Meteyard, L. & Holmes, N. P. TMS SMART - Scalp mapping of annoyance ratings and twitches caused by Transcranial Magnetic Stimulation. *J. Neurosci. Methods* **299**, 34–44 (2018).
26. Di Lazzaro, V., Rothwell, J. & Capogna, M. Noninvasive Stimulation of the Human Brain: Activation of Multiple Cortical Circuits. *Neuroscientist* **24**, 246–260 (2018).
27. Biabani, M. *et al.* The effects of transcranial direct current stimulation on short-interval intracortical inhibition and intracortical facilitation: a systematic review and meta-analysis. *Reviews in the Neurosciences* **29**, 99–114 (2018).
28. Batsikadze, G., Moliadze, V., Paulus, W., Kuo, M.-F. & Nitsche, M. A. Partially non-linear stimulation intensity-dependent effects of direct current stimulation on motor cortex excitability in humans. *J. Physiol. (Lond.)* **591**, 1987–2000 (2013).
29. Hodgkin, A. L. & Huxley, A. F. Currents carried by sodium and potassium ions through the membrane of the giant axon of *Loligo*. *J Physiol* **116**, 449–472 (1952).
30. Moradi Chameh, H. *et al.* Diversity amongst human cortical pyramidal neurons revealed via their sag currents and frequency preferences. *Nat Commun* **12**, 2497 (2021).
31. Faber, D. S. & Pereda, A. E. Two Forms of Electrical Transmission Between Neurons. *Frontiers in Molecular Neuroscience* **11**, 427 (2018).
32. Si, W., Wang, J., Tsang, K. M. & Chan, W. L. Harmonics and intermodulation in subthreshold FitzHugh-Nagumo neuron. *Chaos* **19**, 033144 (2009).

33. Sorkhabi, M. M., Wendt, K & Denison, T. Temporally Interfering TMS: Focal and Dynamic Stimulation Location. *42nd Annual International Conference of the IEEE Engineering in Medicine & Biology Society (EMBC)* (2020).
34. Chaieb, L., Antal, A. & Paulus, W. Transcranial alternating current stimulation in the low kHz range increases motor cortex excitability. *Restor. Neurol. Neurosci.* **29**, 167–175 (2011).
35. Moliadze, V., Antal, A. & Paulus, W. Electrode-distance dependent after-effects of transcranial direct and random noise stimulation with extracephalic reference electrodes. *Clin Neurophysiol* **121**, 2165–2171 (2010).
36. Terranova, C. *et al.* Is There a Future for Non-invasive Brain Stimulation as a Therapeutic Tool? *Front. Neurol.* **9**, (2019).
37. Goldsworthy, M. R. & Hordacre, B. Dose dependency of transcranial direct current stimulation: implications for neuroplasticity induction in health and disease. *J Physiol* **595**, 3265–3266 (2017).
38. Labruna, L. *et al.* Individual differences in TMS sensitivity influence the efficacy of tDCS in facilitating sensorimotor adaptation. *Brain Stimul* **12**, 992–1000 (2019).
39. Labruna, L. *et al.* Efficacy of Anodal Transcranial Direct Current Stimulation is Related to Sensitivity to Transcranial Magnetic Stimulation. *Brain Stimul* **9**, 8–15 (2016).
40. Lu, H., Lam, L. C. W. & Ning, Y. Scalp-to-cortex distance of left primary motor cortex and its computational head model: Implications for personalized neuromodulation. *CNS Neurosci Ther* **25**, 1270–1276 (2019).
41. Nieminen, J. O., Koponen, L. M. & Ilmoniemi, R. J. Experimental Characterization of the Electric Field Distribution Induced by TMS Devices. *Brain Stimul* **8**, 582–589 (2015).
42. Feurra, M. *et al.* State-Dependent Effects of Transcranial Oscillatory Currents on the Motor System: What You Think Matters. *J. Neurosci.* **33**, 17483–17489 (2013).
43. Feurra, M. *et al.* Frequency-dependent tuning of the human motor system induced by transcranial oscillatory potentials. *J Neurosci* **31**, 12165–12170 (2011).

44. Heise, K.-F. *et al.* Evaluation of a Modified High-Definition Electrode Montage for Transcranial Alternating Current Stimulation (tACS) of Pre-Central Areas. *Brain Stimul* **9**, 700–704 (2016).
45. Dissanayaka, T., Zoghi, M., Farrell, M., Egan, G. F. & Jaberzadeh, S. Does transcranial electrical stimulation enhance corticospinal excitability of the motor cortex in healthy individuals? A systematic review and meta-analysis. *Eur. J. Neurosci.* **46**, 1968–1990 (2017).
46. Inukai, Y. *et al.* Comparison of Three Non-Invasive Transcranial Electrical Stimulation Methods for Increasing Cortical Excitability. *Front Hum Neurosci* **10**, 668 (2016).
47. Carroll, T. J., Riek, S. & Carson, R. G. Reliability of the input-output properties of the cortico-spinal pathway obtained from transcranial magnetic and electrical stimulation. *J. Neurosci. Methods* **112**, 193–202 (2001).
48. Kamen, G. Reliability of motor-evoked potentials during resting and active contraction conditions. *Med Sci Sports Exerc* **36**, 1574–1579 (2004).
49. Malcolm, M. P. *et al.* Reliability of motor cortex transcranial magnetic stimulation in four muscle representations. *Clin Neurophysiol* **117**, 1037–1046 (2006).
50. Horvath, J. C., Forte, J. D. & Carter, O. Evidence that transcranial direct current stimulation (tDCS) generates little-to-no reliable neurophysiologic effect beyond MEP amplitude modulation in healthy human subjects: A systematic review. *Neuropsychologia* **66**, 213–236 (2015).